The Molecular Structures of Pyridine-Chromiumpentacarbonyl and Bis(pyridine)-Chromiumtetracarbonyl

WOLFGANG RIES†, IVAN BERNAL*, MICHAEL QUAST and THOMAS A. ALBRIGHT**

Department of Chemistry, University of Houston, Houston, Tex. 77004, U.S.A.

Received June 23, 1983

The structures of pyridinechromiumpentacarbonyl, (1), and bis(pyridine)chromiumtetracarbonyl,(2) have been determined. (1) crystallizes in the space group Pbam *with* a = *15.289(3)* Å, b = *19.276(5)* Å *and* c = *7.677(6)* Å. *(2) crystallizes in the space group* $P\bar{1}$ *with* a = *7.365(2)* Å, b = *8.136(2)* Å, c = *13.491(4)* Å, α = *89.49(2)°*, β = *88.89(2)°*, *and* γ = *63.09(2)°*. *The structures refined to* R_w *values of 0.020 and 0.034 for (1) and (2), respectively. In both cases the pyridine rings are planar and stagger the* cis *Cr–CO bonds. A comparison of the structural results from these two compounds to piperidinechromiumpentacarbonyl and* $Cr(CO)_6$ *seems to indicate that the pyridine ligand is a weaker σ-donor and stronger π-acceptor than the saturated analog, piperidine.*

Introduction

In a separate study [1] we have investigated the ability of the optically active ligands 2-methylpiperidine and 3-methylpiperidine to induce rotational strength into the visible-UV electronic transitions of derivatives having general composition $M(CO)_5$(pip) with M = Cr, Mo and W and pip = 2- or 3-methylpiperidine. In order to establish the absolute configurations of the Me-pip ligands and of the metal carbonyl derivatives, we had to determine their structures and it is at this point that we found in the recent literature a report by Cotton *et al.* [2] on the structure of a 'mixed' crystal containing one molecule of $Cr(CO)_5$(piperidine) and a molecule of $Cr(CO)_5$(pyridine). However, this study was disturbing since the geometrical description of the pyridine was not consistent with known information about this molecule nor with our results on the systems described above. Consequently, we decided to study the crystal structures of $Cr(CO)_5$(pyridine) and $Cr(CO)_4$(pyridine)$_2$ whose synthesis has been reported by Dennenberg and Darensbourg [3]. Our results are given together with a suggestion on the origin of the discrepancies in the previous results [2].

Results and Discussion

Description of the Molecules

Both compounds (1) and (2) exist in their respective crystals as discrete molecules. Whereas for (2) all atoms are found in general positions, the crystals of (1) contain two independent half molecules in the asymmetric unit with crystallographically imposed mirror symmetry for each. The chromium atom, the aromatic ring system and the CO ligand *trans* to it are located in the mirror plane and the mutually *trans* carbonyl ligands at general positions.

The coordination geometry for the chromium atoms in (1) is almost an ideal octahedron with the largest deviation therefrom in the angles Cl–Cr1–C2 and C21–Cr2–C22 (Δ = 1.8° and 2.0° respectively). Disregarding the hydrogen positions the largest differences between the two symmetrically independent molecules of (1) are found in the distances Cr–N (Δ = 0.017 Å), Cr–C3 (Δ = 0.017 Å) and C2–O2 (Δ = 0.013 Å) but even those are barely significant. One can, therefore, use averaged values from both molecules of (1) for comparisons of intramolecular bonding parameters with data already published. This is further supported by the fact that both molecules of (1) show almost identical thermal motion, as evidenced from Figs. 1 and 2. Due to molecular symmetry the pyridine rings are perfectly planar, their plane bisecting the angles between the two unique carbonyl ligands and their mirror images.

*Author to whom correspondence should be addressed.

†NATO Postdoctoral Fellow at the University of Houston 1981–1982.

**Camille and Henry Dreyfus Teacher-Scholar, 1980–1982; Alfred P. Sloan Research Fellow, 1982–1984.

0020-1693/84/$3.00

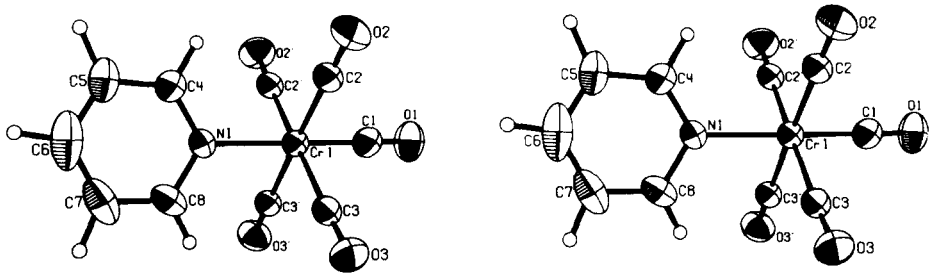

Fig. 1.This is a stereo pair with atoms drawn as 50% probability ellipsoids. Note the mirror plane passing through the molecule, containing the pyridine ring, passing through Cr1, C1 and O1 and mirroring C2–O2 and C3–O3 into C2'–O2' and C3'–O3', respectively.

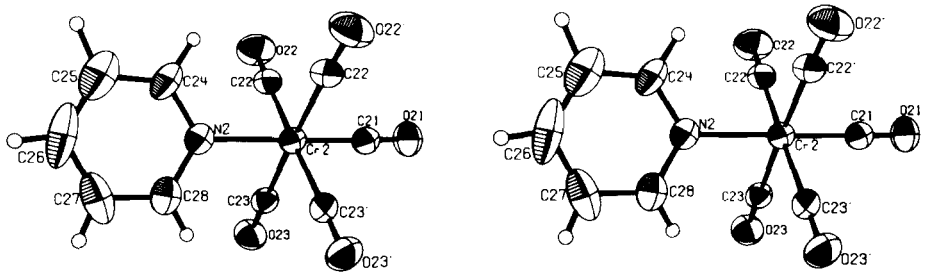

Fig. 2. This is a stereo plot of the second molecule in the asymmetric unit for compound (1). There is also a mirror plane passing through the pyridine ring of this molecule, as described in Fig. 1.

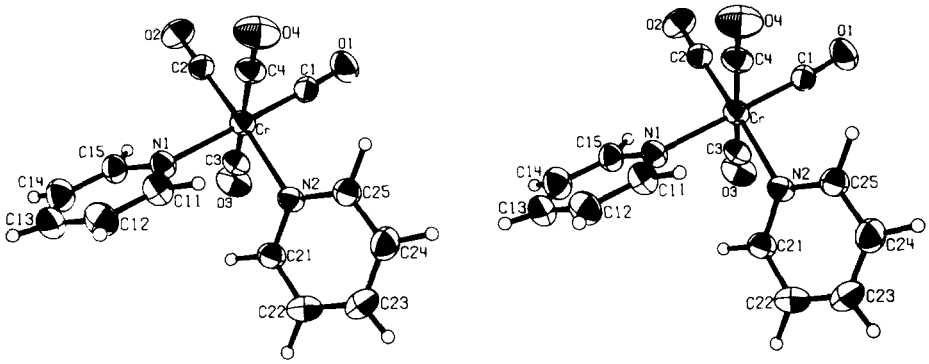

Fig. 3. Stereo plot of molecule (2). Ellipsoids are 50% equi-probability. Note that the pi-bonded pair of electrons (p_z-orbital) on the two nitrogens of the pyridine ligands point half-way between pairs of C–O ligands.

In contrast to (1), the coordination around the metal center in (2) is a slightly distorted octahedron (Fig. 3), the angles N1–Cr–N2 (85.4°) and Cl–Cr–C2 (88.3°) are smaller than the ideal value and the angles N1–Cr–C2 (93.0°) and N2–Cr–C1 (93.5°) increased. In addition the angles N1–Cr–C3 (94.3°) and N2–Cr–C4 (94.2°) angles differ significantly from 90°, resulting a twisting between the $Cr(CO)_4$ fragment and the N1–Cr–N2 moiety, which is illustrated in Fig. 4. The calculation of the mean least-squares planes for the two pyridine ligands (Table VII) demonstrates that both ring systems are planar within the error limit and there is only a minor deviation of the chromium atom from plane B (0.034(1) Å) and none from plane A (–0.002(1) Å).

The molecules of (2) have a non-crystallographic twofold symmetry, which is indicated by the perfect matching of the nonhydrogen atoms in Fig. 5, which was drawn by superimposing a molecule of (2) and its image rotated by 180° around the axis bisecting the N1–Cr–N2 angle. The largest differences after the best fit of both images, as evaluated by BMFIT [4] are Cr–N1 *vs.* Cr–N2 (Δ = 0.013 Å) and C14–C15 *vs.* C24–C25 (Δ = 0.030 Å). As mentioned for

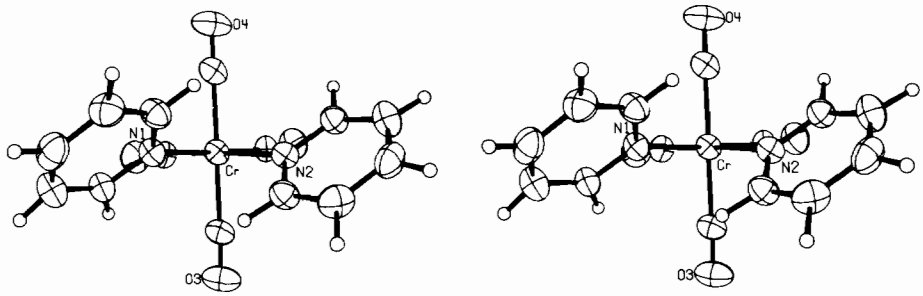

Fig. 4. A different view of molecule (2) emphasizing the relationship between the $Cr(CO)_4$ and the N1–Cr–N2 fragments (see text).

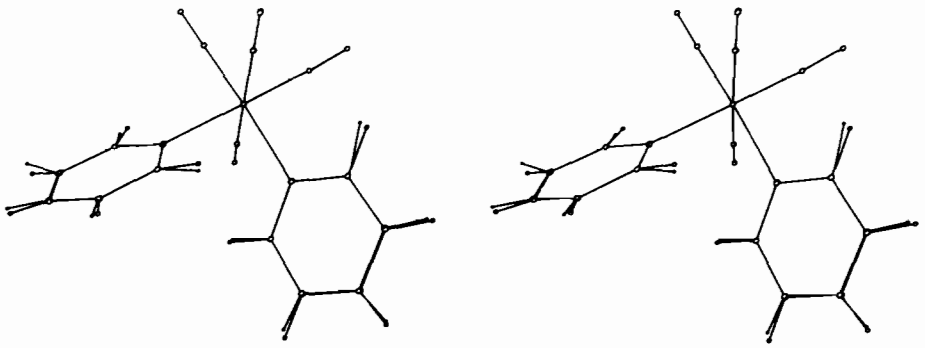

Fig. 5. This is a double stereo plot obtained by plotting the single molecule in the asymmetric unit of compound (2) on top of its rotated image (rotated by 180° about the vector bisecting the N1–Cr–N2 angle). Note that the match is nearly perfect and that the worst deviations occur at the hydrogens of the pyridine ligands (see text).

(1) these differences are not sufficiently significant to distinguish between both pyridine ligands and therefore, when possible, averaged values from both ring systems are used for comparison in the discussion. As evidenced by the torsion angles C2(C3)–Cr–N1–C15 of 40.9° (–46.5°) and Cl-(C4)–Cr–N2–C25 of 40.6° (–47.5°) both aromatic ligands are turned about 3° around the N–Cr bond in the same sense and away from the position in which the planes containing the ring atoms bisect the angles between *cis* substituents at the chromium center.

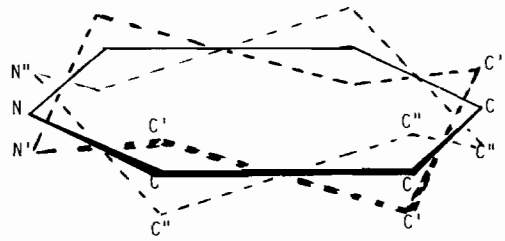

Fig. 6. This figure shows that two piperidine rings, rotated by 180° about the N–C4 axis, each with 50% occupancy, give rise to a flat projection which appears to be a 'pyridine' ring.

Discussion

As already mentioned in the Introduction and providing part of the motivation for this study, is the fact that we are not aware of any structural study of a compound containing pyridine as a ligand coordinated to a zerovalent chromium atom in a molecular coordination compound. Nevertheless, there is one exception which is dealt with in some detail, as it refers to compound (1) of this report. A recent paper [2] reported the coexistence of $(CO)_5CrNC_5H_{10}$ and $(CO)_5CrNC_5H_5$ in one crystal. From their crystallographic data, the authors reported that substitution of piperidine by pyridine does not affect the bonding parameters of the two $(CO)_5CrN$ moieties of these molecules, which indicates identical σ-donor and π-acceptor strength for piperidine and pyridine. This conclusion is difficult to understand given the differences in chemical and physical properties for those two ligands in the uncoordinated state. A careful examination of the data published for the 'mixture' of $(CO)_5CrPip$ and $(CO)_5CrPy$ (Pip = C_5H_{10}, Py = C_5H_5) in the same crystal and comparison with those presented in this paper reveal two interesting aspects: (*a*) in contrast to the $(CO)_5CrPip$ molecule in the 'mixture', which

is well behaved, the $(CO)_5CrPy$ molecule shows high thermal parameters for almost all nonhydrogen atoms. (*b*) the average C–N and C–C distances for the pyridine ring system in the 'mixture' are much longer than expected for an aromatic ligand (1.386 Å, 1.442 Å *vs.* 1.34 Å [5], 1.37 Å [5]). We therefore suggest that the planar arrangement of the carbon atoms observed for one molecule of the 'mixture' is not due to the presence of pyridine but to disorder of piperidine ligands in a way depicted in Fig. 6. Simple geometrical calculations show that the C′–C″ distance for disordered positions in a model according to Fig. 6 is only about 0.50 Å and the contraction of C–N and C–C bonds of ideal length (1.48 Å, 1.54 Å) in a chair arrangement to those in an averaged planar arrangement (1.40 Å, 1.46 Å) is consistent with the values observed for the 'pyridine' ligand in the 'mixture'. In addition the orientation of the thermal ellipsoids in the 'pyridine' model is such that they have their largest axis along a vector connecting the two equivalent atoms in a disordered model. There is, therefore, strong evidence that the crystals used in the structure determination of the 'mixture' contained only one species *i.e.* $(CO)_5CrPip$ with two molecules in the asymmetric unit one of them disordered statistically over two opposite chair conformations of the piperidine ring.

The examination of the Cr–C–O distances for (1) and (2) given in Table V shows the expected differences in the Cr–C bond lengths between those CO ligands *trans* to the N-donor and those *trans* to another CO ($\Delta_{(1)}$ = 0.050 Å, $\Delta_{(2)}$ = 0.068 Å). These differences compare favorably with those observed for $(CO)_5CrPip$ (Δ = 0.077 Å) indicating considerably lower σ-donor ability and, perhaps, a higher π-acceptor capability for pyridine than for piperidine, as they are closer to the differences observed for $(CO)_5CrL$ compounds with π-acceptor ligands (L = $P(OCH_3)_3$, Δ = 0.035 Å [6]). The same magnitude of difference is observed for $(CO)_4$-FePy (0.033 Å) and $(CO)_4$Fe-Pyrazine (0.036 Å) [5], but in these two cases the *trans* influence is obscured by the difference in axial or equatorial CO position.

The average Cr–N distance is shorter in (1) and (2) than the one found for $(CO)_5CrPip$ ($\Delta_{(1)}$ = 0.047 Å, $\Delta_{(2)}$ = –0.039 Å) reflecting the change in nitrogen hybridization. The influence of metal coordination on the pyridine ring geometry is not significant as all distances and angles are close to the ideal values.

The orientations of the pyridine planes in compounds like (1) and (2), when staggered or eclipsed with respect to the *cis* ligands, can be determined by two separate forces. As can be seen in the structure of $(C_{10}H_8N_2)(C_5H_5N)(CO)_3Mo$ [7] the Mo–N distance for the bipyridyl ligand eclipsed to the *cis* carbonyl ligands [2.235(7) Å], is significantly shorter than the Mo–N distance for the pyridine ligand [2.311(9) Å] which is in a staggered conformation. This seems to indicate better metal d-orbital overlap with the aromatic N-donor ligands when in an eclipsed conformation. In (1), calculations show that upon rotation of the pyridine ligand about the Cr–N vector the nonbonding distances between the hydrogen at the 2-position and the adjacent *cis* carbonyl substituent are the following: Using an idealized model derived from the bonding parameters of (1) ($\sphericalangle$Cr–N–C = 120°, $\sphericalangle$N–C–H = 120°, d_{CrN} = 2.15 Å, d_{NC} = 1.35 Å, d_{CH} = 1.00 Å) the distance H(2-Py)–C(CO) increases from 2.34 Å in an eclipsed conformation to 2.78 Å in the staggered ring conformation. Therefore, hydrogens in the 2-position of the pyridine ligand strongly favor a staggered conformation, which minimizes repulsive interactions. The fact that in (1) and (2) the pyridine planes are almost or perfectly bisecting the angles between subsituents in *cis* coordination sites demonstrates that the conformation of (1) and (2) is mainly determined by steric forces. This is consistent with the observation that no preferred conformation is found for pyridine type ligands in trigonal bipyramidal complexes [5]. These arguments above are further supported by the observed deviations from ideally bisecting orientations for the pyridine planes in (2). Replacement of one carbonyl ligand in compound (1) by a nitrogen donor, with an increased chromium ligand distance and a slightly smaller Van der Waals radius at the donor site, reduces non-bonded contacts to the α-hydrogen from this site. As a result, the pyridine planes in (2) should be twisted about the Cr–N bond so as to bring H11 and H21 closer to N2 and N1 respectively. This is clearly documented in the Table VIII which shows the torsion angles: C11–N1–Cr–N2 (45.1°) and C15–N1–Cr–C2 (40.9°) significantly smaller than the related angles C11–N1–Cr–C4 (–49.2°) and C15–N1–Cr–C3 (–46.5°). The same is true for the second pyridine system in (2) (45.9° and 40.6° vs. –48.5° and –47.5°). Even though the steric considerations mentioned above are sufficient to understand most of the conformational relationships, they are not very useful in explaining the twisting of the $Cr(CO)_4$ moiety *vs.* the $Cr(NC_5H_5)_2$ portion of the molecule. As can be seen in Fig. 4 and the packing diagram (Fig. 8) this process increases, if at all CO–H interactions.

Experimental

All procedures were carried out under a N_2 atmosphere or a Vacuum Atmospheres dry box. Pyridine was distilled and deoxygenated just prior to its use. THF was distilled over Na/benzophenone. Irradia-

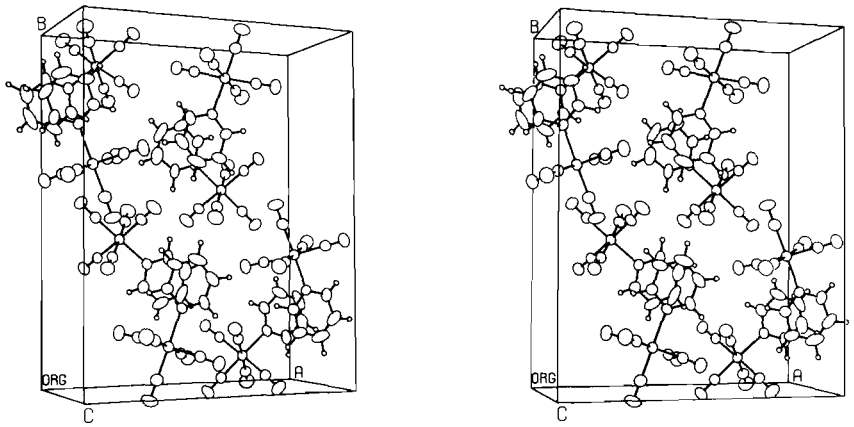

Fig. 7. Packing diagram for compound (1). This is a stereo plot.

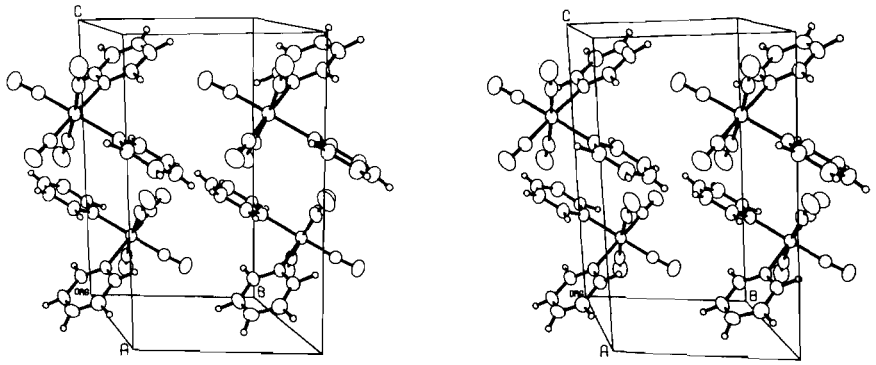

Fig. 8. Packing diagram for compound (2). This is also a stereo plot.

tions were carried out with a Hanovia 450-W medium pressure ultraviolet lamp.

Preparation of $Cr(CO)_5Py$ (1)

Chromium hexacarbonyl (2 g) was dissolved in 500 ml of THF and irradiated at 0 °C for approximately 3.5 h at which time there was no further evolution of CO. Pyridine (3 ml) was added to the solution and the reaction mixture was stirred at room temperature for 0.5 h. The THF was removed under vacuum and the solid products were sublimed to remove any unreacted $Cr(CO)_6$. The remaining solid consisted of largely the mono-substituted product along with a small amount of the di-substituted product. The mono-substituted product was separated by dissolving it in hexane. Slow evaporation of the hexane solution and cooling to 0 °C yielded bright yellow crystals of $Cr(CO_5)Py$; m.p. 95–96 °C, lit [2] 96 °C; IR: ν_{CO} 2080, 1990, 1940, 1920 cm^{-1}.

Preparation of $Cr(CO)_4Py_2$, (2)

$Cr(CO)_4Py_2$ was prepared in a similar fashion except that in this case 5 ml of pyridine was added before irradiation and the photolysis was carried out at room temperature. The product was recrystallized from a mixture of THF and hexane at 0 °C yielding orange crystals; m.p. 162–163 °C (uncor) with decomp., lit [2] 172 °C with decomp.; IR: ν_{CO} 2010, 1895, 1878, 1832 cm^{-1}.

X-Ray Data Collection

The crystals used for this study were prismatic with approx. dimensions of 0.6 × 0.2 × 0.2 mm for (1) and 0.5 × 0.3 × 0.2 mm for (2). Since the process of data collection was almost identical for both compounds, the following describes in detail the procedures applied for (1) mentioning those for (2) only in case they differ.

The crystal selected for data collection was mounted on an X–Y–Z translation head and onto

TABLE I. Atomic Coordinates and Thermal Parameters (x1000, Cr x 10000).

Atom	x/a	y/b	z/c	*U*11	*U*22	*U*33	*U*12	*U*13	*U*23
Cr1	0.38896(6)	0.12162(5)	0.50000(0)	418(6)	427(6)	523(7)	−5(5)	0(0)	0(0)
Cr2	0.29413(6)	0.42400(5)	0.00000(0)	406(6)	440(6)	490(7)	−24(6)	0(0)	0(0)
O1	0.3165(3)	−0.0229(2)	0.5000(0)	109(4)	48(3)	107(4)	−19(3)	0(0)	0(0)
O2	0.2548(2)	0.1562(2)	0.2219(4)	65(2)	92(2)	84(3)	7(2)	−27(2)	1(2)
O3	0.5202(2)	0.0806(2)	0.2180(4)	63(2)	81(2)	79(3)	6(2)	17(2)	−11(2)
O21	0.1474(3)	0.5272(2)	0.0000(0)	62(3)	63(3)	93(4)	19(2)	0(0)	0(0)
O22	0.3783(2)	0.5128(2)	0.2782(4)	102(3)	81(2)	80(3)	−25(2)	−14(2)	−21(2)
O23	0.2004(2)	0.3387(1)	0.2768(4)	63(2)	70(2)	83(3)	−6(2)	20(2)	14(2)
N1	0.4394(3)	0.2266(2)	0.5000(0)	42(3)	43(3)	42(3)	−5(3)	0(0)	0(0)
N2	0.4013(3)	0.3519(2)	0.0000(0)	44(3)	54(3)	44(3)	2(3)	0(0)	0(0)
C1	0.3443(4)	0.0327(3)	0.5000(0)	63(5)	53(4)	66(5)	3(4)	0(0)	0(0)
C2	0.3063(2)	0.1444(2)	0.3260(6)	44(3)	51(3)	62(3)	−4(2)	0(3)	0(3)
C3	0.4721(2)	0.0967(2)	0.3235(6)	44(3)	47(3)	60(4)	−2(2)	−3(2)	0(3)
C4	0.3850(4)	0.2813(3)	0.5000(0)	56(5)	48(4)	60(5)	1(4)	0(0)	0(0)
C5	0.4121(6)	0.3492(4)	0.5000(0)	97(7)	46(5)	68(5)	−15(5)	0(0)	0(0)
C6	0.5001(8)	0.3618(4)	0.5000(0)	157(10)	57(7)	58(6)	−39(7)	0(0)	0(0)
C7	0.5566(6)	0.3084(5)	0.5000(0)	74(7)	92(7)	90(7)	−42(6)	0(0)	0(0)
C8	0.5256(4)	0.2411(4)	0.5000(0)	41(5)	80(6)	62(5)	−10(5)	0(0)	0(0)
C21	0.2025(4)	0.4872(3)	0.0000(0)	47(4)	51(4)	58(5)	−2(4)	0(0)	0(0)
C22	0.3482(3)	0.4787(2)	0.1743(6)	53(3)	49(3)	57(3)	−7(2)	−4(3)	−1(3)
C23	0.2366(2)	0.3709(2)	0.1745(6)	39(2)	50(3)	58(3)	−1(2)	3(2)	−5(3)
C24	0.4849(4)	0.3724(4)	0.0000(0)	35(4)	91(7)	77(6)	8(5)	0(0)	0(0)
C25	0.5551(6)	0.3290(6)	0.0000(0)	60(7)	137(9)	93(7)	19(8)	0(0)	0(0)
C26	0.5407(7)	0.2602(7)	0.0000(0)	74(7)	168(12)	67(6)	72(9)	0(0)	0(0)
C27	0.4563(8)	0.2360(5)	0.0000(0)	120(9)	64(7)	68(6)	40(7)	0(0)	0(0)
C28	0.3884(5)	0.2832(4)	0.0000(0)	56(5)	68(5)	58(5)	11(5)	0(0)	0(0)
H4	0.316(3)	0.271(2)	0.500(0)	8(2)					
H5	0.363(4)	0.389(3)	0.500(0)	13(3)					
H6	0.513(4)	0.410(3)	0.500(0)	10(2)					
H7	0.622(4)	0.312(3)	0.500(0)	9(3)					
H8	0.568(3)	0.204(2)	0.500(0)	6(2)					
H24	0.494(4)	0.426(2)	0.000(0)	9(2)					
H25	0.618(4)	0.352(3)	0.000(0)	13(3)					
H26	0.579(4)	0.226(3)	0.000(0)	8(3)					
H27	0.440(3)	0.194(2)	0.000(0)	5(2)					
H28	0.333(3)	0.268(2)	0.000(0)	3(2)					

TABLE II. Atomic Coordinates and Thermal Parameters (x1000).

Atom	x/a	y/b	z/c	*U*11	*U*22	*U*33	*U*12	*U*13	*U*23
Cr1	0.1346(1)	0.2307(1)	0.2500(1)	382(5)	351(5)	521(6)	−130(4)	−8(4)	−8(4)
O1	0.2022(6)	0.5296(5)	0.1521(3)	82(3)	57(3)	83(3)	−39(3)	1(3)	14(2)
O2	−0.2318(6)	0.5299(5)	0.3488(3)	56(3)	58(3)	82(3)	−4(2)	12(2)	−14(2)
O3	−0.1501(6)	0.2605(5)	0.0852(3)	77(3)	72(3)	88(4)	−34(3)	−38(3)	9(3)
O4	0.3895(6)	0.2634(5)	0.4154(3)	68(3)	72(3)	91(4)	−24(3)	−32(3)	−13(3)
N1	0.1024(7)	0.0127(5)	0.3283(3)	42(3)	39(3)	54(3)	−18(2)	−2(3)	4(2)
N2	0.3864(6)	0.0100(5)	0.1721(3)	41(3)	37(3)	53(3)	−17(2)	−3(2)	−2(2)
C1	0.1753(8)	0.4117(7)	0.1873(4)	47(4)	45(4)	50(4)	−21(3)	5(3)	0(3)
C2	−0.0889(9)	0.4117(7)	0.3125(4)	52(4)	44(4)	51(4)	−19(3)	4(3)	−2(3)
C3	−0.0414(8)	0.2430(7)	0.1469(4)	46(4)	37(3)	60(4)	−17(3)	−14(3)	7(3)
C4	0.2991(8)	0.2422(7)	0.3545(5)	41(4)	36(3)	67(5)	−13(3)	−1(3)	−8(3)
C11	0.2651(9)	−0.1360(8)	0.3649(4)	44(4)	47(4)	62(4)	−20(3)	−7(3)	7(3)
C12	0.2476(11)	−0.2745(8)	0.4154(5)	63(5)	48(4)	60(5)	−21(4)	−12(4)	14(3)

(continued on facing page)

TABLE II. *(continued)*

Atom	x/a	y/b	z/c	*U*11	*U*22	*U*33	*U*12	*U*13	*U*23
C13	0.0635(12)	−0.2686(9)	0.4294(5)	85(6)	55(5)	56(5)	−40(5)	4(4)	5(4)
C14	−0.1068(10)	−0.1159(9)	0.3948(5)	54(5)	65(5)	76(5)	−32(4)	5(4)	1(4)
C15	−0.0808(9)	0.0179(8)	0.3450(4)	42(4)	47(4)	57(4)	−20(3)	2(3)	4(3)
C21	0.3719(9)	−0.1359(7)	0.1356(4)	48(4)	46(4)	60(4)	−22(3)	−1(3)	−6(3)
C22	0.5288(10)	−0.2764(8)	0.0835(5)	63(5)	41(4)	63(5)	−14(4)	−4(4)	−10(3)
C23	0.7071(10)	−0.2679(9)	0.0694(5)	57(5)	54(4)	49(4)	−10(4)	9(4)	−7(4)
C24	0.7258(9)	−0.1193(9)	0.1044(5)	45(4)	59(4)	74(5)	−19(4)	9(4)	0(4)
C25	0.5626(9)	0.0175(8)	0.1554(4)	45(4)	47(4)	55(4)	−21(3)	1(3)	−4(3)
H11	0.395(6)	−0.130(5)	0.354(3)	5(2)					
H12	0.369(8)	−0.362(7)	0.442(4)	9(2)					
H13	0.033(9)	−0.337(7)	0.464(4)	9(2)					
H14	−0.243(6)	−0.101(6)	0.397(3)	5(2)					
H15	−0.202(8)	0.147(7)	0.308(4)	12(2)					
H21	0.245(7)	−0.146(6)	0.153(3)	6(2)					
H22	0.500(7)	−0.379(6)	0.049(3)	7(2)					
H23	0.792(8)	−0.336(7)	0.025(4)	8(2)					
H24	0.837(7)	−0.086(6)	0.085(3)	6(2)					
H25	0.589(7)	0.127(6)	0.191(3)	8(2)					

TABLE III. Intramolecular Bond Distances (A) for $Cr(CO)_5$-NC_5H_5 (1).

Cr1–N1	2.165(4)	Cr2–N2	2.148(4)
Cr1–C1	1.846(6)	Cr2–C21	1.856(6)
Cr1–C2	1.890(4)	Cr2–C22	1.893(4)
Cr1–C3	1.918(4)	Cr2–C23	1.901(4)
C1–O1	1.152(6)	C21–O21	1.143(6)
C2–O2	1.145(4)	C22–O22	1.132(4)
C3–O3	1.138(4)	C23–O23	1.145(4)
N1–C4	1.342(6)	N2–C24	1.339(7)
N1–C8	1.348(7)	N2–C28	1.340(7)
C4–C5	1.373(8)	C24–C25	1.361(10)
C5–C6	1.366(10)	C25–C26	1.344(12)
C6–C7	1.343(10)	C26–C27	1.371(12)
C7–C8	1.382(9)	C27–C28	1.381(9)
C4–H4	1.07(4)	C24–H24	1.05(5)
C5–H5	1.08(6)	C25–H25	1.06(6)
C6–H6	0.96(5)	C26–H26	0.87(5)
C7–H7	1.01(5)	C27–H27	0.86(4)
C8–H8	0.95(4)	C28–H28	0.90(4)

an Enraf-Nonius computer controlled CAD-4 diffractometer. Mo-Kα radiation was used in conjunction with a dense graphite monochromator crystal, assumed to be ideally imperfect in a parallel arrangement, the take-off angle set at 5.85°. The crystal to source and the crystal to detector distances were fixed at 216 mm and 173 mm respectively. The instrument is equipped with attenuators whose attenuation factors were checked using the diffracted beams from a standard crystal (ammonium rubidium tartrate), provided by the Enraf-Nonius laboratories, with the pulse height analyzer in the counting chain set to receive 90% of the incoming bean. Under the OS/4 operating system [8] the computer is programmed to assume that diffracted beams exceeding 50,000 cps are to be attenuated.

An initial orientation matrix is obtained applying the subroutines SEARCH, SETANG and INDEX, providing in addition the Niggli matrix [9] used in our laboratory in conjunction with the tables by Roof [10] to determine the crystal system and lattice symbol. 25 strong reflections well distributed over the reciprocal sphere and with $30° \leqslant 2\theta \leqslant 40°$ were obtained from a data collection with rapid scans. These were centered carefully to determine the final cell parameters, using LS. Checking symmetry equivalent reflections confirmed the Laue symmetry mmm for (1) which is imposed by the orthogonal lattice. Programming the instrument to scan the zones with possible systematic absences revealed, as discussed in detail later, the space group to be either *Pbam* (No. 55) or *Pba2* (No. 32). Compound (2) showed Laue symmetry $\bar{1}$ and as in the case of (1) the correct space group (*P1* or $P\bar{1}$) had to be determined during refinement. Table IX summarizes the crystallographically important data for (1) and (2).

The diffracted intensities were collected using the $\theta-2\theta$ scan technique with a rapid prescan of about 5°/min with the scan range determined by $\Delta\theta$ = a + btanθ (a = 0.90°, b = 0.35°) and backgrounds measured for 25% of the scanning time on either side of the reflection. The aperture was fixed at a value of 2.5 mm. The equations to determine the net intensity I_n and standard deviation $\sigma(I_n)$ from the total intensity I_{tot} and backgrounds I_{bl} and I_{br} are

TABLE IV. Intramolecular Bond Angles (°) for $Cr(CO)_5$-NC_5H_5(1).[a]

N1–Cr1–C1	179.1(2)	N2–Cr2–C21	179.3(2)
N1–Cr1–C2	91.2(1)	N2–Cr2–C22	91.6(1)
N1–Cr1–C3	89.9(1)	N2–Cr2–C23	90.3(1)
C1–Cr1–C2	88.2(2)	C21–Cr2–C22	88.0(2)
C1–Cr1–C3	90.7(2)	C21–Cr2–C23	90.2(2)
C2–Cr1–C3	90.1(2)	C22–Cr2–C23	90.2(2)
C2–Cr1–C2′	89.9(2)	C22–Cr2–C22′	89.9(2)
C3–Cr1–C3′	89.9(2)	C23–Cr2–C23′	89.6(2)
Cr1–C1–O1	179.9(1)	Cr2–C21–O21	178.5(5)
Cr1–C2–O2	177.7(4)	Cr2–C22–O22	177.8(4)
Cr1–C3–O3	178.4(4)	Cr2–C23–O23	178.3(4)
Cr1–N1–C4	120.9(4)	Cr2–N2–C24	122.5(5)
Cr1–N1–C8	122.8(5)	Cr2–N2–C28	121.8(4)
C4–N1–C8	116.3(6)	C24–N2–C28	115.7(6)
N1–C4–C5	124.2(7)	N2–C24–C25	124.8(8)
C4–C5–C6	117.8(8)	C24–C25–C26	118.6(9)
C5–C6–C7	119.8(8)	C25–C26–C27	119.3(9)
C6–C7–C8	120.0(8)	C26–C27–C28	118.9(8)
C7–C8–N1	122.0(7)	C27–C28–N2	122.7(8)
N1–C4–H4	117(3)	N2–C24–H24	115(3)
C4–C5–H5	118(3)	C24–C25–H25	117(4)
C5–C6–H6	113(4)	C25–C26–H26	129(4)
C6–C7–H7	126(4)	C26–C27–H27	127(4)
C7–C8–H8	118(3)	C27–C28–H28	120(3)

[a]Atom labels marked with ′ refer to positions generated by the crystallographically implied molecular mirror plane.

TABLE V. Intramolecular Bond Distances (Å) for $Cr(CO)_4$-$(NC_5H_5)_2$(2).

Cr–N1	2.158(4)	N2–C21	1.337(6)
Cr–N2	2.171(4)	N2–C25	1.341(6)
Cr–C1	1.828(5)	C21–C22	1.387(7)
Cr–C2	1.834(6)	C22–C23	1.356(8)
Cr–C3	1.891(6)	C23–C24	1.366(8)
Cr–C4	1.906(6)	C24–C25	1.388(7)
C1–O1	1.160(5)	C11–H11	0.98(4)
C2–O2	1.159(5)	C12–H12	0.93(5)
C3–O3	1.128(5)	C13–H13	0.82(5)
C4–O4	1.130(6)	C14–H14	0.96(4)
N1–C11	1.357(6)	C15–H15	1.15(5)
N1–C15	1.344(6)	C21–H21	1.00(4)
C11–C12	1.366(7)	C22–H22	1.07(4)
C12–C13	1.344(8)	C23–H23	0.86(5)
C13–C14	1.391(8)	C24–H24	1.00(4)
C14–C15	1.358(7)	C25–H25	1.11(5)

$$I_n = I_{tot} - 2(I_{bl} + I_{br})$$

$$\sigma(I_n) = [I_{tot} + 4(I_{bl} + I_{br})]^{1/2}$$

Reflections with $I_n \leq 0$ are rejected as weak, those with $I_n > 0$ rescanned at a rate such that $I_n/\sigma \geq 1.9$. In order to check the alignment of the crystals one

TABLE VI. Intramolecular Bond Angles (°) for $Cr(CO)_4$-$(NC_5H_5)_2$(2).

N1–Cr–N2	85.4(2)	C11–C12–C13	120.0(6)
N1–Cr–C1	176.8(2)	C11–C12–H12	114(4)
N1–Cr–C2	93.0(2)	C13–C12–H12	126(4)
N1–Cr–C3	94.3(2)	C12–C13–C14	118.5(6)
N1–Cr–C4	89.3(2)	C12–C13–H13	129(4)
N2–Cr–C1	93.5(2)	C14–C13–H13	112(4)
N2–Cr–C2	176.3(2)	C13–C14–C15	119.1(6)
N2–Cr–C3	89.8(2)	C13–C14–H14	125(3)
N2–Cr–C4	94.2(2)	C15–C14–H14	115(3)
C1–Cr–C2	88.3(2)	C14–C15–N1	123.3(6)
C1–Cr–C3	88.7(2)	C14–C15–H15	128(3)
C1–Cr–C4	87.8(2)	N1–C15–H15	108(3)
C2–Cr–C3	87.1(2)	N2–C21–C22	123.2(6)
C2–Cr–C4	89.0(2)	N2–C21–H21	117(3)
C3–Cr–C4	174.8(2)	C22–C21–H21	120(3)
Cr–C1–O1	176.7(5)	C21–C22–C23	118.8(6)
Cr–C2–O2	177.5(5)	C21–C22–H22	119(3)
Cr–C3–O3	176.2(5)	C23–C22–H22	122(3)
Cr–C4–O4	174.6(5)	C22–C23–C24	119.3(6)
Cr–N1–C11	122.0(4)	C22–C23–H23	119(4)
Cr–N1–C15	121.8(4)	C24–C23–H23	119(4)
Cr–N2–C21	122.1(4)	C23–C24–C25	119.0(6)
Cr–N2–C25	121.0(4)	C23–C24–H24	125(3)
C11–N1–C15	116.2(5)	C25–C24–H24	115(3)
C21–N2–C25	116.9(5)	C24–C25–N2	122.7(5)
N1–C11–C12	122.9(6)	C24–C25–H25	117(3)
N1–C11–H11	113(3)	N2–C25–H25	120(3)
C12–C11–H11	124(3)		

TABLE VII. Least-squares Planes, Atomic Deviations (Å) Therefrom and Interplanar Angles (°) for $Cr(CO)_4(NC_5H_5)_2$.

A Plane defined by N1, C11, C12, C13, C14, C15
$-0.1549x - 0.4817y - 0.8625z + 4.008 = 0$

Cr	−0.002(1)	C12	−0.009(6)
C1	0.052(5)	C13	0.014(7)
O1	−0.151(4)	C14	−0.009(7)
N1	0.006(4)	C15	−0.001(6)
C11	−0.001(6)		

B Plane defined by N2, C21, C22, C23, C24, C25
$-0.1571x + 0.4886y - 0.8582z + 2.409 = 0$

Cr	0.034(1)	C22	0.008(6)
C2	0.104(5)	C23	−0.009(6)
O2	0.198(4)	C24	0.003(6)
N2	−0.007(4)	C25	0.005(6)
C21	0.000(6)		

C Plane defined by Cr, N1, N2, C13, C23
$-0.7218x - 0.0000y - 0.6921z + 3.711 = 0$

	max deviation	N2	0.008(5)

(continued on facing page)

TABLE VII. *(continued)*

D Plane defined by Cr, O1, O2, C1, C2
$-0.6497x + 0.0025y - 0.7602z + 3.794 = 0$

	max deviation	C1	0.025(6)

E Plane defined by Cr, N1, N2, C1, C2
$-0.6945x - 0.0027y - 0.7194z + 3.753 = 0$

Cr	−0.002(1)	C1	−0.056(6)
O1	−0.149(4)	C2	0.056(6)
O2	0.125(4)	C13	−0.125(8)
N1	−0.049(5)	C23	0.140(7)
N2	0.050(5)		

F Plane defined by Cr, N1, C1, C3, C4
$0.5365x - 0.6855y - 0.4922x + 1.801 = 0$

Cr	0.016(1)	C1	0.042(6)
O1	0.024(4)	C3	−0.045(6)
O3	−0.127(4)	C4	−0.047(6)
O4	−0.150(4)	C13	0.066(7)
N1	0.033(4)		

G Plane defined by Cr, N2, C2, C3, C4
$0.5390x + 0.6835y - 0.4922z - 0.521 = 0$

Cr	−0.010(1)	C2	−0.046(6)
O2	−0.028(4)	C3	0.047(6)
O3	0.138(4)	C4	0.044(6)
O4	0.155(4)	C23	−0.025(7)
N2	−0.036(4)		

Dihedral angles:

A,B	58.1	A,C	44.9	A,D	41.0	A,E	43.2
A,F	47.8	A,G	89.3	B,C	45.0	B,D	40.9
B,E	43.5	B,F	89.8	B,G	47.8	C,D	5.7
C,E	2.2	C,F	92.7	C,G	92.8	D,E	3.5
D,F	88.6	D,G	88.5	E,F	91.0	E,G	91.3
F,G	86.4						

TABLE VIII. Selected Intramolecular Torsion Angles (°) for $Cr(CO)_4(NC_5H_5)_2$(2).

C1–Cr–N1–C11	−24.3	C2–Cr–N2–C21	−16.8
C1–Cr–N1–C15	154.7	C2–Cr–N2–C25	161.0
C2–Cr–N1–C15	40.9	C1–Cr–N2–C25	40.6
C3–Cr–N1–C15	−46.5	C4–Cr–N2–C25	−47.5
C4–Cr–N1–C11	−49.2	C3–Cr–N2–C21	−48.5
N2–Cr–N1–C11	45.1	N1–Cr–N2–C21	45.9
N2–Cr–C2–O2	−82.4	N1–Cr–C1–O1	−53.4
C3–Cr–C4–O4	−8.1	C4–Cr–C3–O3	9.5

reflection [6, 11, 2 for (1); 1, 3, 9 for (2)] was recentered after every 200 reflections measured showing no significant deviation from the position calculated from the final orientation matrix. To test the stability of the crystal and the reliability of the counting chain two reflections [11, 2, 1 and 6, 11, 2 for (1); 1, 2, 9 and 5, 5, 3 for (2)] were monitored after every 2 hrs. of X-ray exposure time. Neither (1) nor (2) showed significant decay in intensity for the standards with deviations less than 3% from the mean.

Data decoding was accomplished using a locally written program. Lorentz and polarization factors were applied in converting the intensities to structure factor amplitudes, $|F_o|$. The polarization expression used for crystal monochromatized radiation was that given by Kerr and Ashmore [11]. No corrections for absorption were made due to the low values of the absorption coefficients ($\mu_{(1)}$ = 10.83 cm^{-1}, $\mu_{(2)}$ = 8.46 cm^{-1}). Standard deviations in the structure factor amplitudes $\sigma(|F_o|)$ were estimated as $\sigma(|F_o|) = \sigma(I)/(2Lp|F_o|)$.

TABLE IX. Comparison of Bond Lengths (A) and Angles (°) for $Cr(CO)_4L_2$, L = CO, Py, Pip.[a]

	$Cr(CO)_6$	$Cr(CO)_5Py$	$Cr(CO)_4Py_2$	$Cr(CO)_5Pip$
Cr–N		2.157	2.165	2.204
$Cr–C_t$[b]	1.915(2)	1.851	1.831	1.824
$Cr–C_c$[c]		1.901	1.899	1.901
$C_t–O_t$[b]	1.140(3)	1.148	1.160	1.162
$C_c–O_c$[c]		1.140	1.129	1.136
N–C		1.342	1.345	1.481
C–C		1.365	1.370	1.510
$Cr–C_t–O_t$[b]		179.2	177.1	177.7
$Cr–C_c–O_c$[c]		178.1	175.4	174.9

[a]If possible the values are averaged for all chemically equivalent bonds. [b]C_t, O_t refer to the positions *trans* to the N-donor ligand. [c]C_c, O_c refer to the positions *cis* to the N-donor.

TABLE X. Summary of Data Collection and Processing Parameters.

	$Cr(CO)_5NC_5H_5$ (1)	$Cr(CO)_4(NC_5H_5)_2$ (2)
Space Group	*Pbam*	$P\bar{1}$
Cell Constants	a = 15.289(3) Å	a = 7.365(2) Å
	b = 19.276(5) Å	b = 8.136(2) Å
	c = 7.677(6) Å	c = 13.491(4) Å
		α = 89.49(2)°
		β = 88.89(2)°
		γ = 63.09(2)°
Cell Volume	V = 2262.54 Å^3	V = 720.80 Å^3
Molecular Formula	$C_{10}H_5CrNO_5$	$C_{14}H_{10}CrN_2O_4$
Molecular Weight	271.151	322.243
Density (calc.)	ρ = 1.5918 g cm^{-3} (z = 8)	ρ = 1.4845 g cm^{-3} (z = 2)
Radiation	Mo-Kα (λ = 0.71069 Å)	
Absorption Coefficient	μ = 10.83 cm^{-1}	μ = 8.46 cm^{-1}
Data Collection Range	$4° \leq 2\theta \leq 56°$	$4° \leq 2\theta \leq 53°$
Scan Width	$\Delta\theta = (0.90 + 0.35 \tan\theta)°$	
Maximum Scan Time	240 sec	240 sec
Scan Speed Range	0.35 to 5.03° min^{-1}	
Total Data Collected	3125	2972
Data with $I > 3\sigma(I)$	1085	1520
Total Variables	211	230
$R = \Sigma \lvert\lvert F_o\rvert - \lvert F_c\rvert\rvert / \Sigma \lvert F_o\rvert$	0.0255	0.0363
$R_w = [\Sigma w^2(\lvert F_o\rvert - \lvert F_c\rvert)^2 / \Sigma w^2 \lvert F_o\rvert^2]^{1/2}$	0.0200	0.0338
Weights	$0.3455/\sigma^2$	$0.5408/\sigma^2$
Goodness of fit	0.56	1.13

Solution and Refinement

All further data processing and calculations were carried out using the SHELX-76 [12] system of programs and MULTAN 72 [13]. The space group assigned to (1), *Pbam*, and proven as the correct choice by successful solution and refinement of the structure, requires one formula unit per asymmetric unit of (1). The Patterson function indicated the presence of two independent half molecules; therefore, we resorted to direct methods (MULTAN 72) from which the positions of the two chromium atoms, together with the positions for the carbon and oxygen atoms of the mutually *trans* CO groups were derived.

The position of the metal center in (2) was determined from a three dimensional Patterson map. Successive difference Fourier syntheses revealed all nonhydrogen atoms. Isotropic, full matrix least-squares refinement converged at R = 0.0647 (0.0835), R_w = 0.0556 (0.0733) for (1) [(2)] with the unweighted and weighted agreement factors R and R_w determined as listed in Table X and R_w minimized during all least-squares refinements. At this stage, all hydrogen atoms were located from difference Fourier maps and refined isotropically, while all nonhydrogen atoms were allowed to refine anisotropically. Table X lists the final agreement factors for (1) and (2) after convergence (shift/esd $\leq$ 0.06 for all parameters) together with the resulting number of parameters and unique contributing reflections used in least-squares. Final difference Fourier maps were featureless with largest peaks of 0.2 e Å^{-3} and 0.35 e Å^{-3} for (1) and (2) respectively. The atomic scattering curves of Cromer and Mann [14] were used for the nonhydrogen atoms and the curve of Steward *et al.* [15] for hydrogen. Corrections for the real and imaginary terms of the anomalous dispersion for Cr were applied using the values given in the International Tables of X-Ray Crystallography [16].

The estimated standard deviations for the positional parameters were computed from the inverse matrix of the final, full matrix, least-squares cycle. No unusually high correlations were noted between any variables in the final cycles. Final atomic coordinates and thermal parameters are presented in Tables I and II. Interatomic distances and angles are given in Tables III to VI. The equations of the least-squares planes through selected groups of atoms for com-

pound (2) are listed in Table VII and selected torsion angles in Table VIII.

The stereo drawings (Figs. 1, 3–5, 7, 8) were obtained with Johnson's ORTEP [17]. The comparisons of molecular geometry were accomplished by BMFIT [4].

Determination of Space Groups

The initial search for systematic absences for (1) revealed the following conditions, referring to the final setting of the crystal axis: 0 k 1 (k = 2n + 1), h 0 1 (h = 2n + 1), 0 0 1 (1 = 2n + 1). As can be seen in the International Tables for X-Ray Crystallography, there is no space group with the symbol $Pba2_1$. Therefore, at least one of the observed types of absences had to be caused by additional molecular symmetry, not imposed by the symmetry elements for the correct space group of (1).

As the number of axial extinctions along *c* was small compared to the zonal extinctions caused by the glide planes the former were assumed to be caused accidentally. The remaining absences were consistent with space group No. 55, *Pbam*, or its noncentrosymmetric counterpart No. 32, *Pba2*. The distribution of normalized structure factors calculated by NORMAL [13] clearly indicated the centrosymmetric choice to be correct. This is supported by the application of Hamilton's *R*-test [18] with the quotient of the weighted agreement factors for refinement to convergence in *Pbam* (R_w = 0.0200) and *Pba2* (R_w = 0.0191) being significantly smaller than the rejectance limit proposed by Hamilton (R_{obs} = 1.05, $R_{136,738,0.50}$ = 1.10) for even 50% probability. Finally, the variance in lengths of chemically equivalent bonds was considerably smaller in *Pbam*. *Pba2*: Δ_{CrC} = 0.126 Å, d_{avCrC} = 1.900 Å; *Pbam*: Δ_{CrC} = 0.028 Å, d_{avCrC} = 1.901 Å), despite the fact that the mean values where the same for both refinements. The same arguments led to our final choice of $P\bar{1}$ for (2).

The packing diagram for (1) (Fig. 7) illustrates the orientation of the molecules in the unit cell and shows the contents of one unit which is helpful in understanding the nature of the axial extinctions for 0 0 1, 1 ≠ 2n. The equation for the structure factors in *Pbam* [19]

$$A = 8 \cos 2\pi\left(hx + \frac{h+k}{4}\right) \cos 2\pi\left(ky - \frac{h+k}{4}\right)$$

$$\cos 2\pi lz; B = 0$$

is reduced for h = o and k = o to

$$A = 8 \cos 2\pi lz; B = 0$$

Assuming two *identical* molecules with mirror symmetry, one in the plane x y 0 and one in the plane x y ½, there is one atom with $z = ½ - z'$ for every atom with $z = 0 + z'$ i.e. the off mirror atoms. Thus for 1 = 2n + 1 the sum of A's over all atoms of the molecule around x y 0 as mirror plane always equals the negative sum of A's over all atoms for the second molecule around plane x y ½, resulting in a zero value for the structure factor amplitudes. This relationship would be destroyed by introducting atoms at general positions (x y z; z ≠ 0, ¼, ½) or by making the off mirror parts of the two molecules non-equivalent. Therefore the observation of these absences lend further support for our model.

Acknowledgements

We thank NATO and the Robert A. Welch Foundation for support of this research.

References

1 I. Bernal, J. D. Korp and J. Mills, to be published.
2 F. A. Cotton, D. J. Darensbourg, A. Frang, B. W. S. Kolthammer, D. Reed and J. L. Thompson, *Inorg. Chem., 20,* 4090 (1981).
3 R. J. Dennenberg and D. J. Darensbourg, *Inorg. Chem., 11,* 72 (1973).
4 L.-K. Liu, BMFIT, University of Texas, Austin (1977), based upon S. C. Nyburg, *Acta Crystallog. B, 30,* 251 (1974).
5 F. A. Cotton and J. Troup, *J. Am. Chem. Soc., 96,* 3438 (1974).
6 H. J. Plastas, J. M. Steward and S. O. Grim, *Inorg. Chem., 12,* 265 (1973).
7 A. Griffith, *J. Cryst. Mol. Struct., 1,* 75 (1971).
8 'Instruction Manual, CAD-4 System', Enraf-Nonius, Delft (Nov. 1977).
9 P. Niggli, 'Kristallographische und Strukturtheoretische Grundbegriffe, Handbuch der Experimentalphysik', Band 7 Teil 1, Akademische Verlagsgesselschaft, Leipzig (1928), S108.
10 R. B. Roof, Jr., A. 'Theoretical Extension of the Reduced Cell Concept in Crystallography', Los Alamos Scientific Report LA-4038 (1969).
11 K. A. Kerr and J. P. Ashmore, *Acta Cryst. A30,* 176 (1974).
12 G. M. Sheldrick, 'SHELX–76, A Program for Crystal Structure Determination', Cambridge University, Cambridge (1976).
13 P. Main, M. N. Woolfson, L. Lessinger, G. Germain and J. P. Declerq, 'MULTAN 72 – A System of Computer Programs for the Automatic Solution of Crystal Structures from X-Ray Diffraction Data', Universities of York, U.K. and Louvain, Belgium (1973).
14 D. Cromer and J. Mann, *Acta Cryst., A24,* 321 (1968).
15 R. F. Stewart, E. R. Davison and W. T. Simpson, *J. Chem. Phys., 42,* 3175 (1965).
16 'International Tables for X-Ray Crystallography', Kynoch Press, Birmingham, Vol. IV (1978) p. 148.
17 C. K. Johnson, ORTEP 2 – A Fortran Ellipsoid Plotting Program for Crystal Structure Illustration', ORNL-5138, Oak Ridge, Tenn. (1972).
18 W. C. Hamilton, *Acta Cryst., 18,* 502 (1965).
19 'International Tables for X-Ray Crystallography', Kynoch Press, Birmingham, Vol. I (1965) p. 404.